

## RED CELLS, IRON, AND ERYTHROPOIESIS

*Plasmodium falciparum* exploits CD44 as a coreceptor for erythrocyte invasion

Barbara Baro,<sup>1,\*</sup> Chi Yong Kim,<sup>1,\*</sup> Carrie Lin,<sup>1</sup> Angel K. Kongsomboonvech,<sup>1</sup> Marilou Tetard,<sup>1</sup> Nana Ansuah Peterson,<sup>1</sup> Nichole D. Salinas,<sup>2</sup> Niraj H. Tolia,<sup>2</sup> and Elizabeth S. Egan<sup>1,3,4</sup>

<sup>1</sup>Department of Pediatrics, Stanford University School of Medicine, Stanford, CA; <sup>2</sup>Host-Pathogen Interactions and Structural Vaccinology Section, Laboratory of Malaria Immunology and Vaccinology, National Institute of Allergy and Infectious Diseases, National Institutes of Health, Bethesda, MD; <sup>3</sup>Department of Microbiology and Immunology, Stanford University School of Medicine, Stanford, CA; and <sup>4</sup>Chan Zuckerberg Biohub–San Francisco, San Francisco, CA

## KEY POINTS

- Human CD44 is dispensable for erythropoiesis.
- *P falciparum* exploits CD44 as a coreceptor for invasion that facilitates signaling to the host cell cytoskeleton.

The malaria parasite *Plasmodium falciparum* invades and replicates asexually within human erythrocytes. CD44 expressed on erythrocytes was previously identified as an important host factor for *P falciparum* infection through a forward genetic screen, but little is known about its regulation or function in these cells, nor how it may be used by the parasite. We found that CD44 can be efficiently deleted from primary human hematopoietic stem cells using CRISPR/Cas9 genome editing, and that the efficiency of ex vivo erythropoiesis to enucleated cultured red blood cells (cRBCs) is not affected by lack of CD44. However, the rate of *P falciparum* invasion was reduced in CD44-null cRBCs relative to isogenic wild-type control cells, validating CD44 as an important host factor for this parasite. We identified 2 *P falciparum* invasion ligands as binding partners for CD44, erythrocyte binding antigen 175 (EBA-175) and EBA-140 and demonstrated that their

ability to bind to human erythrocytes relies primarily on their canonical receptors, glycophorin A and glycophorin C, respectively. We further show that EBA-175 induces phosphorylation of erythrocyte cytoskeletal proteins in a CD44-dependent manner. Our findings support a model in which *P falciparum* exploits CD44 as a coreceptor during invasion of human erythrocytes, stimulating CD44-dependent phosphorylation of host cytoskeletal proteins that alter host cell deformability and facilitate parasite entry.

## Introduction

Malaria due to the apicomplexan parasite *Plasmodium falciparum* is a leading cause of morbidity and mortality in the developing world.<sup>1</sup> The clinical symptoms of malaria occur when the parasites invade and replicate in erythrocytes (red blood cells [RBCs]) in exponential cycles lasting ~48 hours. Asexual replication is critical to disease pathogenesis, and a major focus of intervention efforts. Yet, emerging drug resistance and the lack of a strongly effective vaccine remain major obstacles to malarial control. A deeper understanding of the host–pathogen interactions occurring during the blood stage of this complex parasitic life cycle is needed to advance new therapeutic or preventive strategies.<sup>2–5</sup>

*P falciparum* follows a multistep process for successful erythrocyte invasion, including apical reorientation, host cell deformation, and formation of a moving junction.<sup>6</sup> The driving force for internalization is powered by the parasite's actino-myosin motor. Like other invasive parasites within the phylum Apicomplexa, *P falciparum* merozoites harbor 2 major secretory organelles at their apical tip, the micronemes and the rhoptries,

in which a variety of invasion proteins are localized. Secreted ligands from the erythrocyte binding–like (EBL) and reticulocyte binding protein homologs (PfRh) protein families bind to specific receptors on the erythrocyte, including glycophorin A (GYPA), GYPB, GYPC, and complement receptor 1 (CR1).<sup>2–5</sup> Erythrocyte binding antigen 175 (EBA)-175 and EBA-140 are *P falciparum* EBL ligands that interact with RBCs by binding to GYPA and GYPC, respectively.<sup>2,7–14</sup> Binding occurs through the region II (RII) of each EBA protein, which consists of 2 Duffy binding–like domains.<sup>9,13–15</sup> The EBL and Rh ligands are considered functionally redundant, and mediate apical reorientation and host cell deformation during attachment.<sup>16</sup> After apical reorientation, the *P falciparum* ligand PfRH5 binds to its receptor, basigin. This interaction has been proposed to result in a pore in the RBC membrane and to be required for rhoptry discharge and formation of the moving junction.<sup>17–19</sup>

Our understanding of the role of erythrocyte host factors during *P falciparum* invasion is limited, in part because of the genetic intractability of these unique cells, which are enucleated. CD44 was recently discovered as a host factor for *P falciparum* through a forward genetic short hairpin RNA screen in cultured

RBCs (cRBCs) derived ex vivo from nucleated hematopoietic stem/progenitor cells (HSPCs).<sup>20</sup> Further evidence for a role of CD44 in invasion was obtained using erythroblasts derived from the cell line JK-1, in which CD44-null JK-1 cells were resistant to invasion by 3 different *P falciparum* strains.<sup>21</sup>

Widely expressed on eukaryotic cells, CD44 exists in several isoforms, but RBCs only express the shortest, standard form (CD44s).<sup>22</sup> Its function in human RBCs is largely uncharacterized aside from encoding the Indian blood group antigens.<sup>23</sup> In other cells, the principal ligand for CD44 is hyaluronic acid (HA); its binding activates cell signaling pathways that modulate the cytoskeleton and influence processes such as cell migration, metastasis, and survival.<sup>24-28</sup> CD44 is a receptor for group A *Streptococcus* on epithelial cells, the binding of which stimulates Rac1, phosphorylation of cellular proteins, and cytoskeletal rearrangements permissive for invasion.<sup>29</sup> Through its cytoplasmic domain, CD44 interacts with Band 4.1 superfamily proteins such as ezrin, radixin, and moesin (ERM).<sup>30,31</sup> These interactions have been shown to lead to the activation of the receptor tyrosine kinase, c-MET, through Ras-MAPK and PI3K-AKT pathways,<sup>32-34</sup> but which downstream effectors are activated by CD44 depend on the stimulus and cell context.<sup>28</sup> CD44 can also function as a coreceptor to help activate receptor tyrosine kinases in cancer cells and during *Listeria* infection of epithelial cells,<sup>34-36</sup> but in neither case are the mechanisms fully understood.

Here, we investigated the function of erythrocyte CD44 during *P falciparum* invasion using a combination of genetic, cell biological, and biochemical approaches. Our findings support a model in which *P falciparum* exploits CD44 as a coreceptor to facilitate its invasion into erythrocytes.

## Methods

### *P falciparum* culture and invasion assays

*P falciparum* strain 3D7 was cultured in deidentified human erythrocytes (Stanford Blood Center) in RPMI 1640 with 25 mM N-2-hydroxyethylpiperazine-N'-2-ethanesulfonic acid, 50 mg/L hypoxanthine, 2.42 mM sodium bicarbonate, and 0.5% Albumax (Invitrogen) at 37°C in 5% CO<sub>2</sub> and 1% O<sub>2</sub>. For invasion assays, schizonts were added at 1.0% to 1.5% parasitemia to RBCs at 0.3% hematocrit in a volume of 100 µL per well. The ring-stage parasitemia was determined after 18 to 24 hours by microscopy of cytopins stained with May-Grünwald and Giemsa stain. A minimum of 1000 enucleated cells were counted blindly for each technical replicate (3 technical replicates per biological replicate).

### Ex vivo erythropoiesis of primary human CD34<sup>+</sup> HSPCs

Generation of cRBCs was performed as previously described, as detailed in "supplemental Methods," available on the *Blood* website.<sup>37</sup> The cells were cocultured at 1 × 10<sup>6</sup> cells per mL on a murine stromal cell layer (MS-5) beginning ~day 14,<sup>38,39</sup> and harvested between days 18 and 20. Enucleation rate was quantified using Vybrant DyeCycle Violet and flow cytometry.

### Genetic modification of primary human CD34<sup>+</sup> cells via CRISPR/CRISPR-associated protein 9 (CRISPR/Cas9)

Two single guide RNAs (sgRNAs) targeting *CD44* were designed using the Genetic Perturbation Platform sgRNA portal of the Broad Institute, and synthesized as chemically modified sgRNAs (Synthego): CD44-Cr1 (GAATACACCTGCAAAGCGGC) and CD44-Cr2 (GCAATATGTGTGCATACTGGG). Ribonuclear proteins (300 pmol of each sgRNA and 200 pmol recombinant Cas9 [rCas9]-nuclear localization signal [NLS]) were introduced on day 2 using a Lonza Amaxa 4-D nucleofector (EO-100). Knockout efficiency was determined by flow cytometry. CD44-null precursors were enriched on day 9 to 11 using CD44 microbeads (Miltenyi).

### Free merozoite assays

Free merozoites were isolated, as previously described.<sup>40</sup> For binding assays, 3 µg of His-tagged rCD44 (rCD44-His), rCD44-Fc, rGYPC-His, or rCD99-Fc were incubated with 200 µL of merozoite suspension for 1 hour at room temperature (RT). Binding was detected by flow cytometry using anti-6x-His, anti-CD99, or anti-CD44 antibodies. For immunofluorescence assays, merozoites were fixed in cold 4% paraformaldehyde/0.0075% glutaraldehyde and incubated with 2 µg of rCD44-Fc for 1 hour at RT. After blocking, they were incubated in anti-RAP1/2 mouse monoclonal and anti-CD44 rabbit polyclonal antibodies followed by goat anti-mouse Alexa Fluor 488 and goat anti-rabbit Alexa Fluor 555.

### Pull-down assays

Schizont-stage lysate from *P falciparum* strain 3D7 was prepared, as described in "supplemental Methods," and incubated with 8 µg of rCD44-Fc (R&D) or recombinant immunoglobulin G-Fc (IgG-Fc; R&D) bound to protein A Dynabeads (Invitrogen) overnight at 4°C. Bound proteins were eluted and submitted to the Stanford University Mass Spectrometry facility for identification, or processed for immunoblotting as described in "supplemental Methods."

### Recombinant protein binding assays

R11-EBA-175-His and R11-EBA-140-His were expressed and purified as described previously and as detailed in "supplemental Methods."<sup>12,14,15,41</sup> Eight micrograms of rCD44-Fc, IgG-Fc (R&D), rCD44-Fc, or rCD55-Fc (SinoBiological), or no protein were bound to 1.5 mg protein A Dynabeads (Invitrogen) for 1 hour at RT. The beads were then incubated with 2 µM R11-EBA-175-His or R11-EBA-140-His in phosphate-buffered saline for 1 hour. In antibody blocking experiments, anti-CD44 BRIC 222 (IBGRL) or BRIC 170 were incubated with rCD44-Fc beads at 50 µg/mL for 1 hour before incubation with the EBA proteins. Binding was detected by flow cytometry using mouse anti-6x His tag antibodies.

### HUDEP-2 experiments

HUDEP-2 cells were cultured and differentiated essentially as previously described, with minor modifications as detailed in "supplemental Methods."<sup>42</sup> Orthochromatic cRBCs were recovered on a Percoll gradient. Genetic modification of the HUDEP-2 cells was performed using CRISPR/Cas9 via

lentivirus transduction or ribonuclear proteins nucleofection, with confirmation of clones by flow cytometry and sequencing. For binding assays,  $1 \times 10^6$  HUDEP-2 cRBCs were incubated in rRII EBA175-His or rRII EBA-140-His at  $5 \mu\text{M}$  in Dulbecco modified Eagle medium with 10% fetal bovine serum and 100 mM NaCl. Binding was detected by flow cytometry using mouse anti-6x His mouse antibody.

### Proteomic analysis and mass spectrometry

Isogenic wild-type (WT) and CD44-CRISPR cRBCs were generated from primary human HSPCs, and CD44-null cRBCs were isolated using microbeads. For each simulation,  $2 \times 10^8$  day-20 cRBCs at 50% hematocrit were incubated with RII-EBA-175 or RII-EBA-140 ( $2 \mu\text{M}$ ) for 30 minutes, followed by lysis in 5 mM sodium phosphate (pH, 8.0) with protease and phosphatase inhibitors. Ghost samples were sent to Applied Biomics, Inc for 2-dimensional difference gel electrophoresis (2D-DIGE) analysis (Hayward, CA), as detailed in "supplemental Methods." Spot picking for mass spectrometry was performed by Applied Biomics based on differential intensity in stimulated vs unstimulated samples in WT vs CD44-null backgrounds.

### Data analysis

All flow cytometry data were analyzed using FlowJo (version 10.6.1). The DeCyder analysis was performed by Applied Biomics using the DeCyder 2D software from GE Healthcare, version 6.5; <http://biotech.gsu.edu/core/Documents/Manuals/decyder-v6.5-manual.pdf>. For statistical analysis of the invasion assays, 2-tailed Student *t* tests were performed using GraphPad Prism version 9.

## Results

### Efficient generation of CD44-null cRBCs from primary human HSPCs

To begin to characterize the role of CD44 in *P. falciparum* invasion, we generated CD44-null RBCs using CRISPR/Cas9 genome editing in primary human HSPCs followed by ex vivo erythropoiesis (Figure 1A). Nucleofection of ribonucleoprotein complexes containing CD44-targeting sgRNAs and recombinant Cas9 resulted in an efficiency of CD44 knockout of ~75% (Figure 1B). Both CD44-CRISPR and control WT populations of erythroid progenitors demonstrated a high rate of proliferation, and progressed through morphologically distinct basophilic,

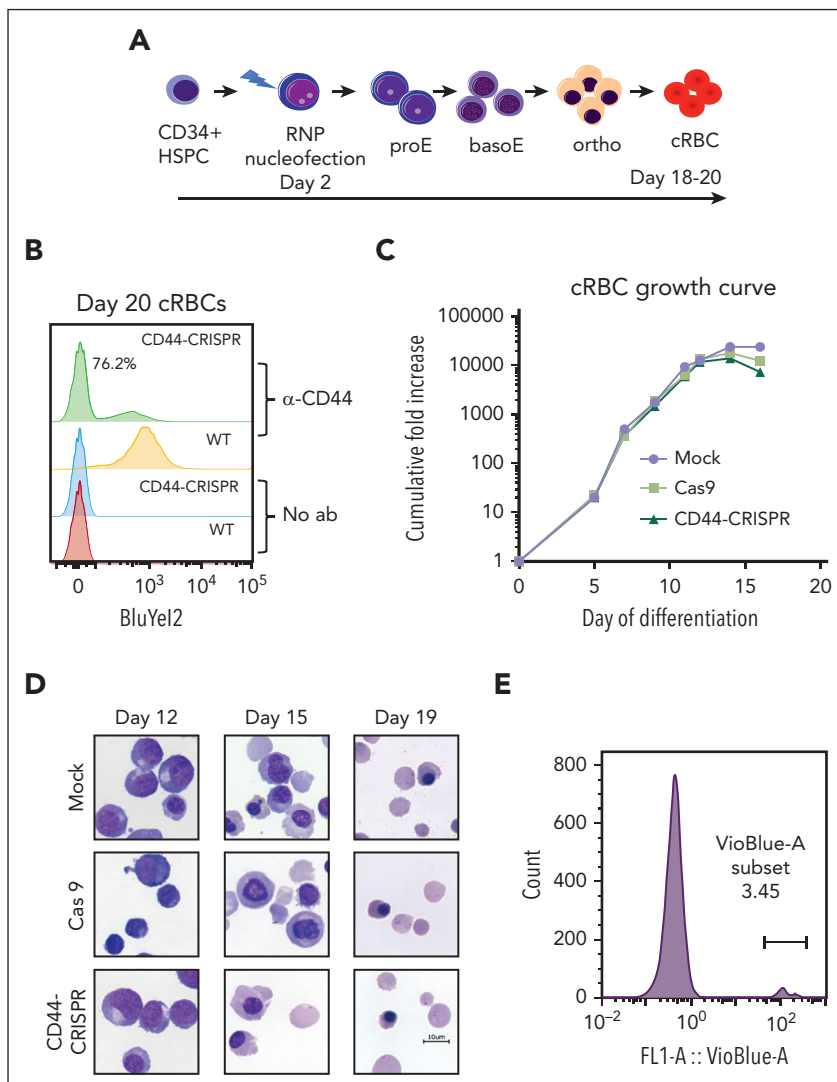


**Figure 1. CD44 is dispensable for erythroid differentiation of primary human HSPCs.** (A) Schematic of genome editing strategy to generate CD44-null cRBCs from primary human CD34<sup>+</sup> HSPCs using CRISPR/Cas9.

Ribonucleoprotein (RNP) complexes consisting of rCas9 and 2 CD44-targeting sgRNAs were introduced by nucleofection on day 2 of culture. Differentiating erythroblasts were plated on a murine stromal cell layer on day ~13 to 14 to facilitate recovery of enucleated cRBCs. (B) Flow cytometry analysis of CD44 surface expression in unmodified (WT) cRBCs, or an isogenic population that was nucleofected with RNPs targeting CD44 (CD44-CRISPR). Anti-CD44 antibody BRIC 222 (IBGRL) was used at a ratio of 1:10 000 followed by goat anti-mouse IgG-PE (1:2000). (C) Representative growth curves of primary human CD34<sup>+</sup> HSPCs during ex vivo erythropoiesis. Nucleofection was performed on day 2 to generate CD44-CRISPR cells, Cas9 control cells (WT cells nucleofected with rCas9 only), or mock control cells (non-transfected). (D) Cytospin images of CD44-CRISPR vs isogenic WT erythroid cells during the time course of ex vivo erythropoiesis. Cas9, nucleofected with Cas9 only; Mock, nontransfected; scale bar, 10 μm. (E) Representative experiment showing enucleation rate of CD44-null cRBCs upon terminal differentiation, as detected by flow cytometry using the cell-permeable DNA stain Vybrant DyeCycle Violet.

polychromatic, and orthochromatic erythroblast stages during terminal differentiation (Figure 1C-D; supplemental Figure 1). Importantly, these cells also underwent efficient enucleation, reproducibly generating >95% enucleated cRBCs (Figure 1D-E). Together, these findings indicate that CD44 can be efficiently deleted from primary human HSPCs, and is not required for ex vivo erythropoiesis or enucleation.

### Impaired *P. falciparum* invasion into CD44-null cRBCs

To investigate the requirement for erythrocyte CD44 in *P. falciparum* invasion, we performed invasion assays using the isogenic WT and CD44-CRISPR-mutant cRBCs. *P. falciparum* 3D7 was synchronized to the schizont stage and incubated with the CD44-CRISPR or isogenic WT cRBCs for ~18 hours to allow for egress and invasion, and the parasitemia was quantified by blinded counts of cytopsin slides. We observed ~50% reduced parasitemia in the CD44-CRISPR population relative to the WT cRBCs, confirming that *P. falciparum* infection is impaired in the absence of CD44 ( $P = .0062$ ; Figure 2A). Visual inspection of the ring-stage parasites growing in WT vs CD44-CRISPR cRBCs did not reveal any gross morphological differences between the 2 genetic backgrounds (Figure 2B). Although most infected cells harbored 1 or 2 parasites, occasional cells with multiple rings

could be detected in both CD44-CRISPR and isogenic WT cRBCs. To determine whether CD44 is essential for *P. falciparum* invasion, we used negative selection to isolate a purer population of CD44-null cRBCs for use in invasion assays (Figure 2C). Again, we observed a moderate invasion phenotype in the CD44-null cRBCs relative to isogenic control cells ( $P = .0010$ ; Figure 2D). Together, these results confirm that CD44 is necessary for efficient *P. falciparum* invasion of erythrocytes but suggest that it is not essential for invasion.

### Direct interaction between *P. falciparum* merozoites and erythrocyte CD44

Given that CD44 has a large extracellular domain and is required for efficient *P. falciparum* infection of cRBCs, we hypothesized that it may act as a receptor for parasite invasion. To investigate this, we isolated free merozoites and quantified their interaction with recombinant CD44 using flow cytometry-based assays (Figure 3A-B). Recombinant GYPC and recombinant CD99 served as positive and negative controls, respectively, with GYPC being a known receptor for *P. falciparum*, and with available evidence suggesting that CD99 plays no role in *P. falciparum* invasion.<sup>8,20</sup> Free merozoites were observed to bind directly to rCD44-Fc but not to rCD99-Fc, confirming that the interaction observed with rCD44-Fc was not attributable to the

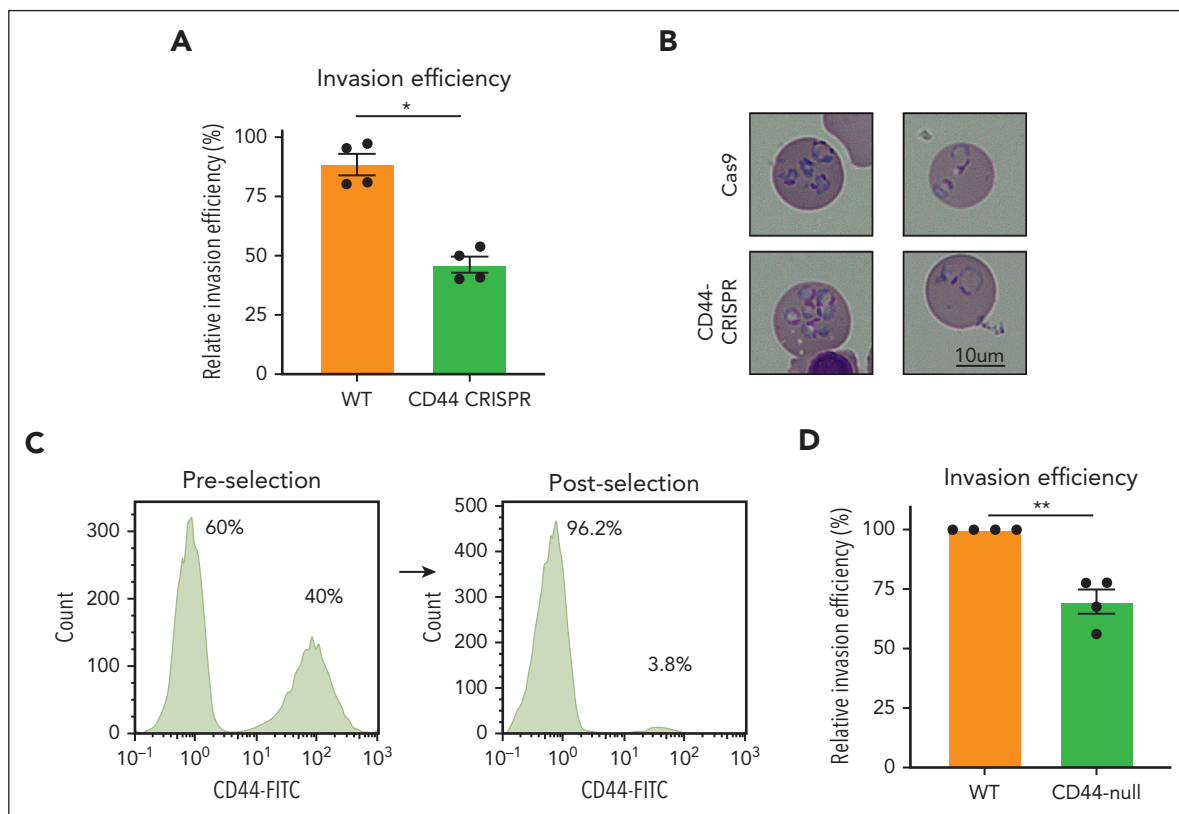


**Figure 2. CD44 is required for efficient *P. falciparum* invasion.** (A) Invasion assays of *P. falciparum* strain 3D7 into WT cRBCs vs CD44-CRISPR cRBCs. Approximately 18 hours after incubation with late-stage schizonts, parasitemia was determined by blinded counting of cytopsin slides stained with May-Grünwald and Giemsa stain, and is presented relative to parasitemia in control erythrocytes. Plotted are 4 biological replicates, each of which was performed in triplicate, with the line indicating the mean  $\pm$  standard error of the mean (SEM); \* $P = .0062$ , 2-tailed paired t test. (B) Cytopsin images of *P. falciparum* parasites ~18 hours after invasion into isogenic WT or CD44-CRISPR cRBCs. (C) Flow cytometry plot showing efficiency of negative selection for CD44-null cRBCs using CD44 microbeads. Anti-CD44 antibody BRIC 222 (IBGRL) was used at 1:10 000 followed by goat anti-mouse IgG-488 (1:1500). (D) Invasion assays of *P. falciparum* strain 3D7 into WT cRBCs vs CD44-null cRBCs isolated by negative selection. Parasitemia was determined by blinded counting of cytopsin slides by 2 individuals, and is presented normalized to the parasitemia in the WT cRBCs for each replicate. Each of 4 biological replicates are plotted, each of which were performed in triplicate, with the line indicating the mean of the biological replicates,  $\pm$ SEM; \*\* $P = .0010$ , 2-tailed t test.

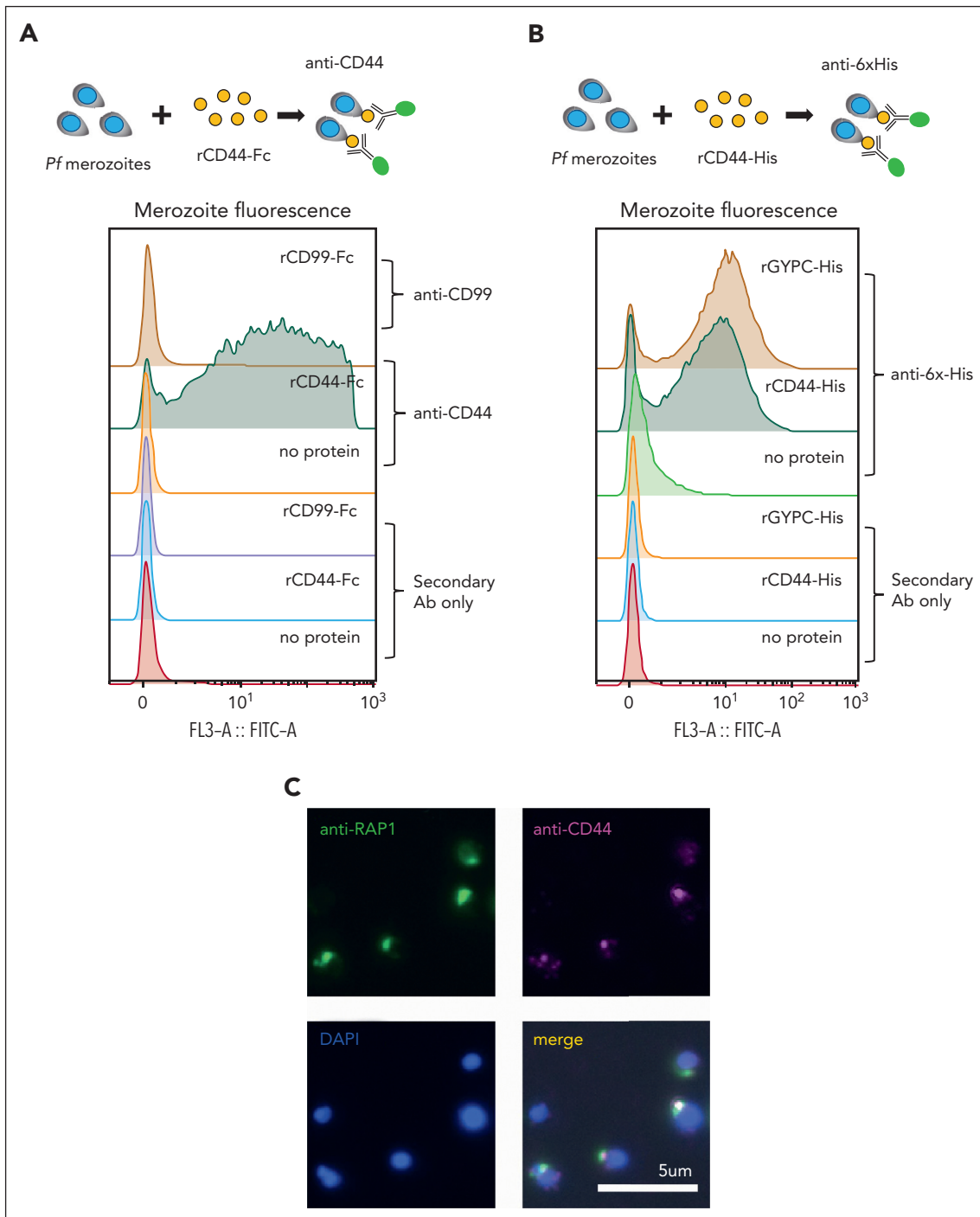


**Figure 3. *P. falciparum* merozoites bind to CD44.** (A) Flow cytometry–based assay to quantify binding between free *P. falciparum* merozoites and recombinant CD44-Fc or CD99-Fc proteins. Free merozoites were incubated with 3 µg recombinant proteins, and binding was detected using anti-CD44 BRIC 222 (IBGRL, 1:1000) or anti-CD99 (Invitrogen; 1:250) antibodies. (B) Flow cytometry–based assay to quantify binding between free *P. falciparum* merozoites and recombinant His-tagged proteins and detection with anti-6x-His mouse monoclonal antibody (Invitrogen; 1:300). (C) Images of immunofluorescence assays of free *P. falciparum* merozoites after binding to rCD44-His, and its colocalization with the merozoite protein RAP1. RAP1 was detected using anti-RAP1/2 mouse monoclonal antibody (from Anthony Holder; 1:500), and CD44 was detected with anti-CD44 rabbit polyclonal antibody (Invitrogen; 1:500), followed by goat anti-mouse AlexaFluor 488 and goat anti-rabbit AlexaFluor 555. Images were taken with a Keyence BZ-X700 all-in-1 fluorescence microscope at ×100 original magnification under oil immersion.

Fc domain (Figure 3A). Binding was also observed for rCD44-His and the positive control rGYPC-His (Figure 3B). In immunofluorescence assays, CD44 localized to the apical end of merozoites, as indicated by its colocalization with the known apical marker RAP1 (Figure 3C). Notably, many *P. falciparum*

invasion ligands are known to be concentrated at the apical end of the merozoite, from which invasion commences. Together, these results suggest that CD44 can act as a receptor for invasion by interacting with a parasite ligand localized in the apical region of the merozoite.



## CD44 interacts with the *P. falciparum* invasion ligands EBA-175 and EBA-140

To identify *P. falciparum* ligand(s) that interact with CD44, we performed in vitro pull-down assays by incubating rCD44-Fc beads or rIgG<sub>1</sub>-Fc (rFc) beads with lysate from *P. falciparum* schizont-stage parasites, followed by mass spectrometry. This analysis revealed a strong enrichment for 2 *P. falciparum* invasion ligands from the EBA family in the rCD44-Fc pull-down relative to the rFc control condition: EBA-175 and EBA-140 (Figure 4A; supplemental Data Set 1). These results were confirmed by independent pull-down experiments followed by western blots, showing that EBA-175 and EBA-140 were specifically detected in the elution from the pull-down using rCD44-Fc but not with rFc (Figure 4B). Moreover, overlay assays in which immobilized rCD44-Fc and rFc were incubated with spent media from *P. falciparum* culture demonstrated specific binding of EBA-175 and EBA-140 to CD44 (supplemental Figure 2). These findings demonstrate that CD44 can interact with EBA-175 and EBA-140, either directly or indirectly.

RII of EBA-175 and EBA-140 comprise the receptor binding domains.<sup>2</sup> To determine whether EBA-175 and EBA-140 RII interact with CD44 directly, we used rCD44-Fc and rFc-coated beads in in vitro binding assays with recombinant RII-EBA-175-His and RII-EBA-140-His. Binding of the RII-EBA proteins to the beads was measured by flow cytometry. We observed a clear shift in fluorescence for rCD44-coated beads incubated with RII-175-His or RII-140-His, whereas no shift was seen for the rFc-coated beads or beads alone, demonstrating direct interactions between rCD44-Fc and both EBA-140 and EBA-175 (Figure 4C). Importantly, there was no detectable binding to CD55-Fc, another glycosylated erythrocyte membrane protein, further demonstrating the specificity of the observed interactions with rCD44-Fc (Figure 4D; supplemental Figure 3). Additionally, we observed that preincubation of the rCD44-Fc beads with anti-CD44 antibody BRIC 222 inhibited the binding by both EBA-175 and EBA-140, but this was not seen for isotype control antibody BRIC 170 (Figure 4E). Together, these findings indicate that both RII-175 and RII-140 can interact directly and specifically with human CD44.

To determine whether the binding of the EBA proteins to CD44 was dependent on sialic acid, we treated rCD44-Fc with neuraminidase to partially remove sialic acid. We observed a partial reduction in binding of EBA-175 and EBA-140 RII to neuraminidase-treated rCD44-Fc compared with untreated rCD44-Fc (supplemental Figure 4). These results suggest that the interaction between the EBA proteins and rCD44 depends, at least in part, on sialic acid.

## CD44 is not a primary determinant of EBA-175 and EBA-140 binding to the RBC

Because the binding of EBA-175 and EBA-140 to RBCs is known to involve GYPA and GYPC, respectively, we sought to determine how the interactions of EBA-175 and EBA-140 with CD44 may contribute to their RBC binding activity. To test this, we used the immortalized erythroid cell line HUDEP-2,<sup>42</sup> which is readily amenable to genetic manipulation and cloning, and which we found can be differentiated to orthochromatic erythroblasts (orthos) permissive to *P. falciparum* invasion (Figure 5A; supplemental Figure 5).

We generated CD44-, GYPA-, or GYPC-null mutants in HUDEP-2 cells using CRISPR/Cas9 genome editing and confirmed that the mutant clones lacked surface expression of the respective proteins by flow cytometry (supplemental Figure 6). After inducing differentiation down the erythroid lineage to orthos, we used the cells in flow cytometry-based binding assays with recombinant RII-175-His and RII-140-His. The results showed that RII-175 bound to the WT and CD44-null orthos to a similar degree (Figure 5B). Similar results were observed for RII-140, with only a slight reduction in binding noted for the CD44-null orthos (Figure 5B). These findings suggest that CD44 is not a primary determinant of EBA-175 or EBA-140 binding to the HUDEP-2 orthos, particularly in comparison with the glycoporphins. Indeed, in parallel experiments using GYPA-null or GYPC-null HUDEP-2 orthos, we observed that RII-175 and RII-140 binding was substantially dependent on GYPA and GYPC, respectively, consistent with these surface proteins being RBC receptors for EBA-175 and EBA-140 (Figure 5C). Notably, CD44 is a surface protein of low abundance on human erythrocytes, with an estimated copy number of ~10 000 molecules per cell, as compared with ~1 × 10<sup>6</sup> copies of GYPA and ~143 000 of GYPC.<sup>4,43</sup> Conceivably, this low copy number could affect the ability of CD44 to serve as prominent binding receptor relative to the glycoporphins.

Next, we generated double-mutant HUDEP-2 cells (GYPA/CD44-null or GYPC/CD44-null) and used them in binding assays. For RII-175, binding to the GYPA/CD44-null HUDEP-2 orthos was minimally reduced relative to GYPA-null HUDEP-2 orthos. Similarly, binding of RII-140 to GYPC/CD44-null HUDEP-2 orthos was slightly reduced relative to GYPC orthos (Figure 5D). Although these minor shifts are consistent with EBA-175 and EBA-140 being able to bind to CD44, they also confirm that CD44 is not a major determinant of the RBC binding activity of EBA-175 or EBA-140, relative to the glycoporphins. Instead, these findings raise the hypothesis that CD44 may be acting as a coreceptor during *P. falciparum* invasion.

## A role for erythrocyte CD44 in EBA-175-induced signaling

In other cell types, CD44 has been shown to facilitate downstream signaling despite lacking intrinsic kinase activity.<sup>28</sup> For example, CD44 acts as a coreceptor for the ErbB family of receptor tyrosine kinases and for the c-MET receptor, regulating diverse cellular processes.<sup>35,44-46</sup> Because we found that CD44 can interact with EBA-175, and recent work has shown that EBA-175 binding to RBCs induces changes in membrane deformability and cytoskeletal protein phosphorylation,<sup>47,48</sup> we investigated whether CD44 plays a role in signaling in RBCs.

We generated pure populations of WT and isogenic CD44-null cRBCs, incubated them with recombinant EBA-175 or mock stimulus, and performed 2D-DIGE on membrane ghost lysates to measure changes in protein intensity in the 2 genetic backgrounds (Figure 6A). We identified 50 spots with ≥1.3-fold change in intensity in 1 or both genetic backgrounds after stimulation with EBA-175, as quantified by DeCyder analysis (Figure 6B; supplemental Data Set 2). Several proteins appeared to be differentially regulated by EBA-175 in WT vs CD44-null cRBCs, suggesting that CD44 may play a role in the regulation (Figure 6C). Because RBCs cannot perform protein synthesis, these changes likely reflect posttranslational modifications.

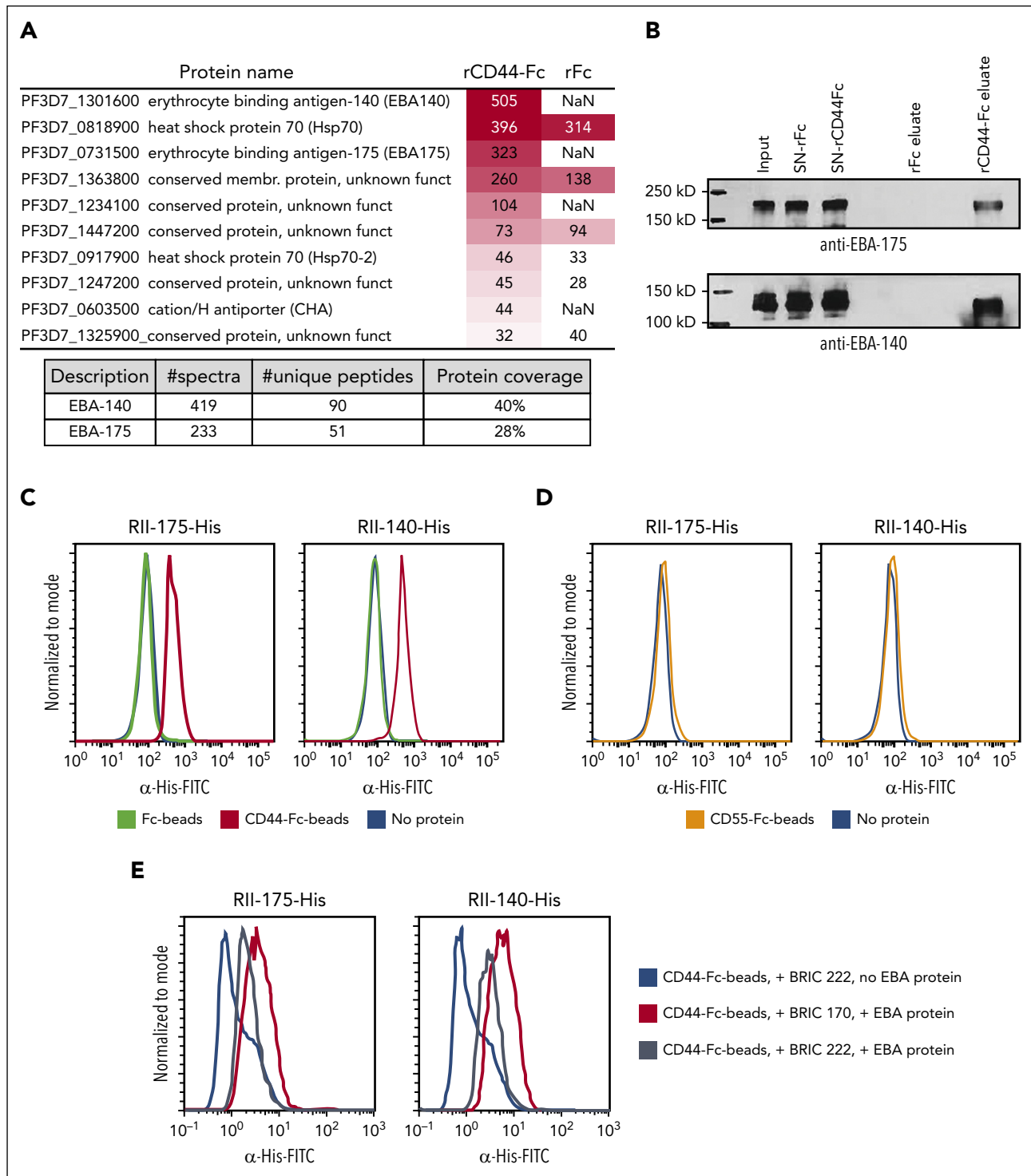


**Figure 4. CD44 specifically interacts with *P. falciparum* invasion ligands EBA-175 and EBA-140.** (A) Mass spectrometry results from affinity purification experiments in which bead-immobilized rCD44-Fc or rFc were incubated with lysate from *P. falciparum* strain 3D7 schizont-stage parasites. The heat map shows the normalized spectral counts (based on protein size) of the most abundant *P. falciparum* proteins detected and their enrichment in rCD44-Fc compared with rFc. NaN indicates “no counts.” The table shows log probability, raw number of spectra, and unique peptides, and coverage of EBA-140 and EBA-175 proteins found in the rCD44-Fc lane. (B) Western blot of independent affinity purification experiment in which bead-immobilized rCD44-Fc or rFc were incubated with *P. falciparum* schizont-stage lysate, followed by immunoblotting for EBA-175 or EBA-140 using anti-EBA-175 or anti-EBA-140 rabbit antisera (from Alan Cowman, 1:2000) followed by goat anti-rabbit-HRP secondary antibody (1:25 000). SN, supernatant. (C) Flow cytometry–based binding assays in which recombinant RII of EBA-175-His (left) or EBA-140-His (right) were incubated with beads coated with rCD44-Fc, rFc, or no protein. Binding was detected using a mouse anti-6x-His IgG antibody (Invitrogen; 1:5000) and goat anti-mouse IgG-FITC (1:1000). (D) Flow cytometry–based binding assays between rCD55-Fc or rFc and RII of EBA-175-His (left) or EBA-140-His (right). (E) Binding assays of RII EBA-175 (left) or RII EBA-140 (right) with rCD44-Fc after incubation of the protein-coated beads with anti-CD44 mouse monoclonal antibody BRIC 222 (50  $\mu\text{g}/\text{mL}$ ) or isotype control BRIC 170, which targets the cytoplasmic domain of Band3 (50  $\mu\text{g}/\text{mL}$ ).

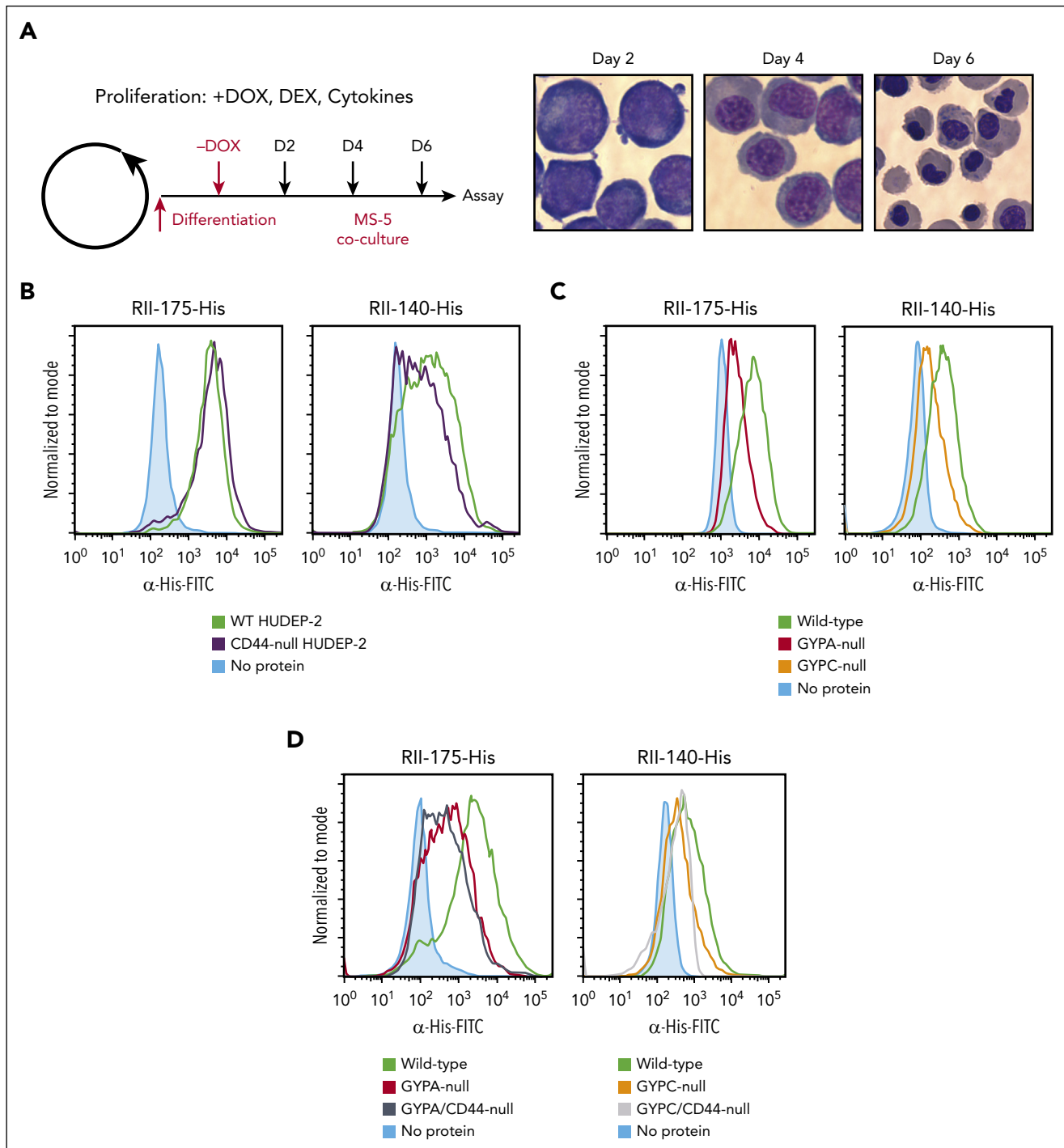


**Figure 5. Genetic analysis in HUDEP-2 cells reveals that GYPA and GYPC are the primary determinants of EBA-175 and EBA-140 binding to cRBCs, respectively.** (A) Schematic of HUDEP-2 proliferation and differentiation protocol, and representative images of differentiating HUDEP-2 cells at  $\times 100$  magnification. Day 2, proerythroblasts; day 4, polychromatic erythroblasts; and day 6, orthos. (B) Flow cytometry–based binding assays of RII regions of EBA-175-His (left) and EBA-140-His (right) incubated with WT vs CD44-null HUDEP-2 orthos. Binding of the EBA proteins to the cells was quantified using anti-His antibody and fluorescent secondary antibody. (C) Flow cytometry–based binding assays of RII regions of EBA-175-His (left) and EBA-140-His (right) incubated with WT, GYPA-null, or GYPC-null HUDEP-2 orthos. Binding was quantified using a mouse anti-6x-His antibody (Invitrogen; 1:300) followed by goat anti-mouse IgG-FITC (1:1000). (D) Flow cytometry–based binding assays of RII regions of EBA-175-His (left) and EBA-140-His (right) incubated with WT, GYPA-null, GYPA/CD44-null, GYPC-null, or GYPC/CD44-null HUDEP-2 orthos. Binding was quantified using the anti-6x-His antibody and fluorescent secondary antibody. DEX, dexamethasone; DOX, doxycycline.

To determine whether these shifts reflected altered protein phosphorylation, we performed 2D-DIGE on ghost lysates from EBA-175–stimulated WT or CD44-null cRBCs using a dye specific for phosphorylated proteins. This analysis identified 26

spots with  $\geq 2$ -fold increased phosphorylation in the stimulated WT cRBC ghost lysate relative to the CD44-null background, indicating that EBA-175–induced phosphorylation of erythrocyte proteins is, at least in part, dependent on CD44



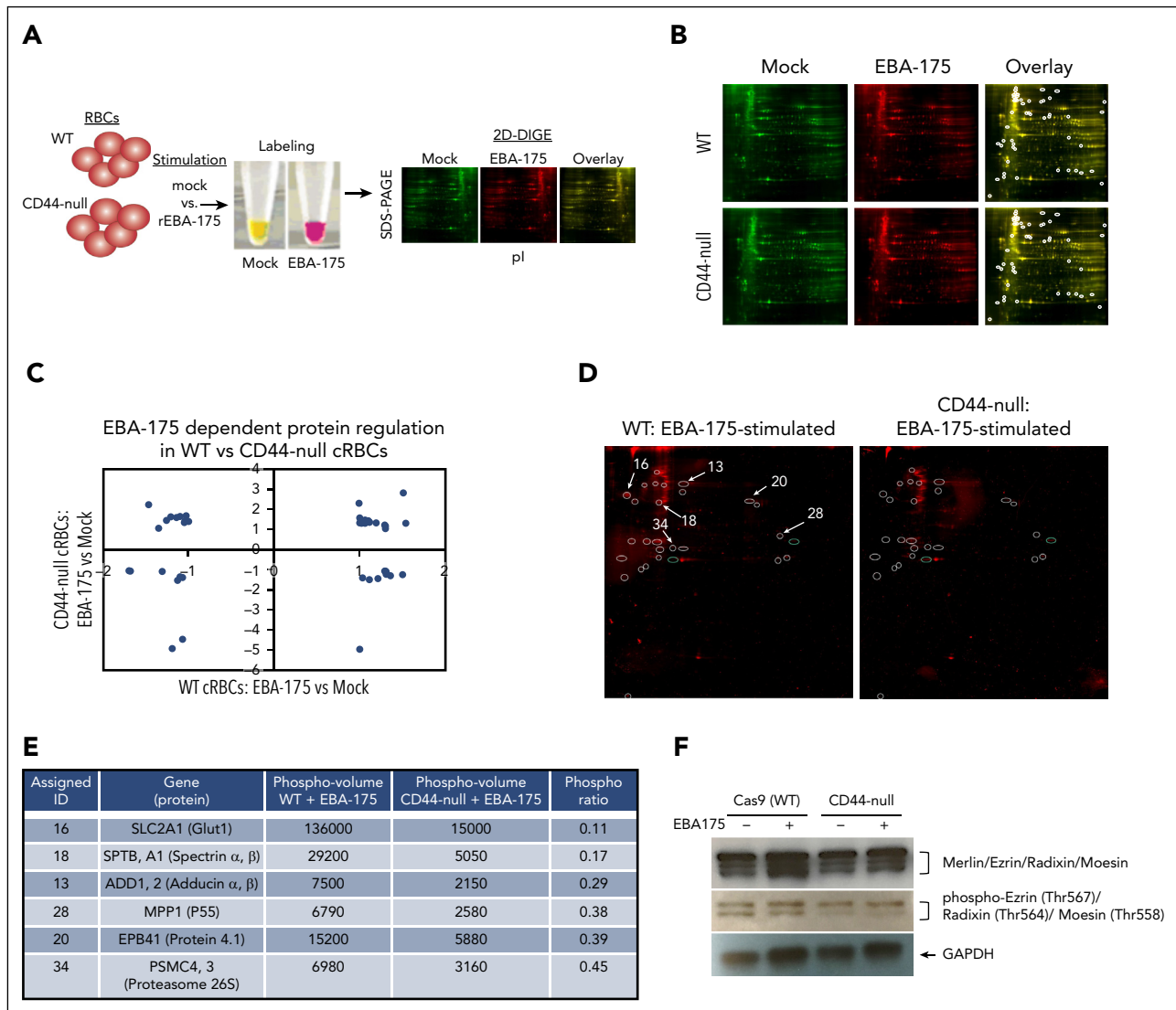


**Figure 6. CD44 facilitates EBA-175-induced signaling to the RBC cytoskeleton.** (A) Schematic of 2D-DIGE assays. (B) 2D-DIGE analysis of WT or CD44-null cRBC lysates stimulated with mock or RII EBA-175. Circles represent spots with  $\geq 1.3$  fold change in intensity in mock- vs RII EBA-175-stimulated samples in 1 or both genetic backgrounds as identified by DeCyder analysis. (C) Quantification of the fold change in intensity in RII EBA-175-stimulated vs mock-stimulated WT cRBCs, and RII EBA-175-stimulated vs mock-stimulated CD44-null cRBCs. Spots identified with  $> 1.3$ -fold change in intensity were plotted. (D) 2D-DIGE analysis of protein phosphorylation in WT vs CD44-null cRBCs stimulated with RII EBA-175. The circles indicate 25 spots with  $\geq 2$ -fold increase in phosphorylation in the stimulated WT cRBCs compared with CD44-null cRBCs. The 6 spots that were sent for identification by mass spectrometry analysis are indicated. (E) High-confidence proteins identified by mass spectrometry with differential phosphorylation between EBA-175-stimulated WT vs CD44-null cRBCs. Phospho-volumes were quantified by Applied Biomics using DeCyder software. (F) Western blot for total and phosphorylated ERM complex proteins (merlin, ezrin, radixin, and moesin) WT or CD44-null cRBCs stimulated with mock or RII EBA-175. Anti-ERM was used at 1:1000, anti-phospho-ERM was used at 1:1000, and anti-GAPDH (1:4000) was used as a loading control, followed by goat anti-rabbit-HRP (1:4000).

(Figure 6D). We chose 6 of the most highly differentially phosphorylated spots between WT and CD44-null ghost lysates for protein identification by mass spectrometry. Interestingly, this analysis identified the cytoskeletal linker protein 4.1, as well as several components of the erythrocyte cytoskeletal network (SLC12A1, adducin  $\alpha/\beta$ , p55, and spectrin  $\alpha/\beta$ ); Figure 6E). Notably, protein 4.1R is a cytoskeletal linker protein that regulates cell shape through its local protein-protein interactions, which include p55,<sup>49-51</sup> and possibly CD44.<sup>52,53</sup> The ERM family members, ezrin, radixin, and moesin, have also been shown to interact with CD44 as cytoskeletal linker proteins.<sup>30,31,54</sup> Although these proteins were not identified in our limited-scope mass spectrometry analysis, immunoblotting for the

ERM proteins demonstrated reduced phosphorylation in CD44-null cRBCs relative to isogenic WT, consistent with a role for CD44 in signaling to the cytoskeleton (Figure 6F).

Because EBA-140 can functionally substitute for EBA-175 to mediate invasion in certain strain backgrounds and we found that both proteins can interact with CD44, we also investigated RII-EBA-140-induced RBC ghost lysate phosphorylation changes and their dependence on CD44 by 2D-DIGE. This analysis showed that stimulation with EBA-140 also leads to altered phosphorylation of several RBC proteins in a CD44-dependent manner, including ankyrin-1, spectrin  $\alpha/\beta$ , and protein 4.1 (supplemental Figure 7).

## Discussion

CD44 is a widely expressed cellular adhesion molecule, affecting diverse cell processes such as migration, inflammatory responses, and metastasis. Its effects are exerted through interactions with ligands (eg, HA), interactions with other surface receptors (eg, c-Met), and interactions with cytoskeletal linker proteins through its conserved cytoplasmic domain.<sup>28,55</sup> Although CD44 has been extensively studied in some cells, little is known about its function on human erythrocytes.<sup>22</sup> Recent evidence suggests that there may be an association between activation of the Gardos channel and the interaction of CD44 with HA, suggesting CD44 may affect erythrocyte senescence.<sup>56,57</sup>

CD44 was first identified as a candidate host factor for *P falciparum* through a pooled, forward genetic short hairpin RNA screen in cultured erythroblasts derived from primary human HSPCs.<sup>20</sup> In the screen, CD44 was one of the top candidates identified, and its importance was validated by the demonstration that *P falciparum* invasion was reduced in CD44-knockdown cRBCs relative to isogenic WT cRBCs. Additional evidence for a role for CD44 in *P falciparum* invasion was reported by Kanjee et al, in which the authors showed that parasite invasion was reduced by ~50% in CD44-knockout cRBCs derived from the JK-1 erythroleukemia line (jkRBCs) as compared with WT jkRBCs.<sup>21</sup> In this work, we report, to our knowledge, for the first time, the efficient generation of CD44-null cRBCs from primary human HSPCs using CRISPR/Cas9 genome editing. Importantly, the cRBCs were observed to proliferate and differentiate normally, demonstrating that CD44 is not required for in vitro erythroid development in human cells. In *P falciparum* invasion assays, we found that parasite invasion was reduced but not completely inhibited in CD44-null cRBCs. This confirms that CD44 plays a role in *P falciparum* invasion but suggests that it is not an essential host factor under these in vitro conditions. This was further assessed by isolating a nearly pure population of CD44-null cRBCs by negative selection. Reduced invasion into the CD44-null cRBCs was again observed, but the phenotype was unexpectedly milder. Variables such as enucleation rate and culture duration could not explain the range in phenotype strength, suggesting that it may be attributable to batch effects and/or CD34<sup>+</sup> donor differences. However, the reproducible reduction in parasite invasion into CD44-null cRBCs vs isogenic WT cRBCs across 8 biological replicates provides strong evidence that CD44 is required for efficient *P falciparum* invasion.

Prior work in epithelial cells created precedent for the idea that CD44 can act as a pathogen receptor. Group A *Streptococcus* binds to CD44 on keratinocytes through its hyaluronic capsule, an interaction that triggers downstream RAC1-dependent signaling and cytoskeletal rearrangements in the host cell, enabling tissue invasion.<sup>29</sup> CD44 on epithelial cells has also been shown to interact with the *Shigella* secreted protein IpaB, leading to cytoskeletal reorganization and increased invasion.<sup>58</sup>

Reasoning that *P falciparum* may exploit CD44 as a receptor for RBC invasion, we used pull-down assays to identify *P falciparum* proteins that interact with CD44. The discovery of EBA-175 and EBA-140 as interactors of CD44 was surprising, because these well-established invasion ligands already have known receptors (GYPA and GYPC, respectively). We confirmed the interactions using multiple methods, including immunoblotting, overlay

assays, recombinant protein binding assays, and cellular binding assays using genetically modified erythroid cells. Of note, the cellular assays demonstrated that GYPA and GYPC are the primary determinants of RII-EBA-175 and RII-EBA-140 binding to RBCs, raising the hypothesis that CD44 may instead be acting as a coreceptor to facilitate invasion. Importantly, in other cells, CD44 has been shown to function as a coreceptor with a variety of proteins, such as c-Met, EGFR, and transforming growth factor  $\beta$ ,<sup>55</sup> and its low surface abundance on RBCs relative to the glycoporphins could be consistent with a coreceptor function. Prior work has shown that the binding affinity of EBA-175 to intact erythrocytes was significantly higher than its affinity to surface-immobilized GYPA<sup>59,60</sup>; our findings may help explain this difference, because the involvement of CD44 might contribute to a stronger binding affinity in native erythrocytes.

The observation that CD44 can interact with both EBA-175 and EBA-140 suggests that it may be interacting with these proteins through a common domain. It is also consistent with prior work demonstrating that diverse *P falciparum* strains rely on CD44 for efficient invasion, despite expressing different dominant invasion ligands.<sup>21</sup> Our finding that the anti-CD44 monoclonal antibody BRIC 222 partially reduced binding of rEBA-175 and rEBA-140 to rCD44 further supports the specificity of these interactions, while also highlighting that the interacting region likely extends beyond the BRIC 222-binding epitope. Interestingly, patient RBC samples deficient in protein 4.1R reportedly have reduced surface expression of CD44 and GYPC, suggesting that these proteins may exist within a complex.<sup>53</sup> Future efforts aimed at mapping the critical residues for binding between CD44 and the EBA proteins will be important for detailed understanding of these interactions, and their relationship with the glycoporphins.

Our results provide evidence for a mechanism in which CD44 acts as a coreceptor for *P falciparum* invasion. A coreceptor role could be consistent with the moderate invasion phenotype observed in the absence of CD44, at least compared with basigin, which is considered an essential receptor for parasite invasion.<sup>17</sup> Coreceptors are generally defined as cell surface molecules that influence receptor-ligand activity but do not contain intrinsic catalytic activity. In the case of *P falciparum* invasion, our results support a model in which EBA protein binding to the RBC surface via the glycoporphins also engages CD44, influencing the phosphorylation of cytoskeletal proteins via interactions between the cytoplasmic domain of CD44 and cytoskeletal linker proteins. Previous work has shown that EBA-175 binding to GYPA increases RBC deformability and is associated with changes in phosphorylation of cytoskeletal proteins.<sup>47,48</sup> EBA-175 shed from merozoites also induces RBC clustering and promotes parasite growth in culture.<sup>41</sup> Because CD44 is an integral membrane protein that can coordinate adhesive and signaling events,<sup>61</sup> our findings provide important insights into how *P falciparum* EBA proteins can signal to the RBC cytoskeleton. Future work will be required to determine whether CD44 is involved in the EBA-175-induced RBC clustering phenotype. Live cell imaging of invasion into CD44-null vs WT cRBCs will also be important next steps to further characterize the CD44-dependent invasion phenotypes. A comprehensive understanding of the signaling pathways triggered during *P falciparum* invasion will also require more extensive investigation, ideally via global phosphoproteomics of genetically altered cRBCs stimulated with actively invading merozoites.

As our understanding of host determinants of infectious diseases advances, novel, host-directed therapies that can counteract the evolution of pathogen resistance are beginning to be brought into clinical practice. Increasing evidence suggests that targeting host factors can be an effective antimalarial strategy.<sup>62-64</sup> Given its role in several disease contexts, CD44 is currently being explored as a therapeutic target, particularly in the oncology field.<sup>65,66</sup> The demonstration in this work that *P falciparum* exploits CD44 to facilitate RBC invasion lays a key foundation for future investigation into the potential of CD44-related pathways as targets for malaria intervention.

## Acknowledgments

The authors thank Ryan Leib and colleagues from the Stanford University Mass Spectrometry Facility, and John Liao from Applied Biomics, Inc (Hayward, CA) for technical assistance. The authors are grateful to members of the Egan Laboratory, John Boothroyd, Ellen Yeh, Paul Bollyky, Michael Eckart, and members of their laboratories for helpful discussions. The authors thank Ryo Kurita and Yukio Nakamura for contributing the HUDEP-2 cell line. Antibodies used in this work were kindly provided by Alan Cowman and Anthony Holder. Some mass spectrometry data were collected at the Vincent Coates Foundation Mass Spectrometry Laboratory, Stanford University Mass Spectrometry (RRID:SCR\_017801).

This work used the Thermo LTQ-Orbitrap Elite mass spectrometer system (RRID:SCR\_018694) that was purchased with funding from National Institutes of Health (NIH) Shared Instrumentation grant S1ORR027425. This work was supported, in part, by NIH, National Cancer Institute grant P30 CA124435 using the Stanford Cancer Institute Proteomics/Mass Spectrometry Shared Resource. This work was supported, in part, by NIH, National Heart, Lung, and Blood Institute grant DP2HL13718601 (E.S.E.), a Bridge Grant Award from the American Society of Hematology (E.S.E.), and a faculty scholar award from the Stanford Maternal Child Health Research Institute (E.S.E.). B.B., A.K.K., and M.T. were funded through postdoctoral fellowships from the Stanford Maternal Child Health Research Institute; and A.K.K. was also supported by a T32 training grant in pediatric nonmalignant hematology and stem cell biology (T32DK098132-06A1). E.S.E. is a Chan Zuckerberg Biohub San Francisco investigator and a Tashia and John Morgridge Endowed Faculty Scholar of the Stanford Maternal and Child Health Research Institute. N.H.T. and N.D.S. are supported by the Intramural Research Program of the NIH, National Institute of Allergy and Infectious Diseases.

## Authorship

Contribution: B.B., C.Y.K., and E.S.E. conceptualized the study; B.B., C.Y.K., C.L., A.K.K., N.A.P., N.D.S., and E.S.E. performed experiments; B.B., C.K., A.K.K., M.T., and E.S.E. performed data analysis; B.B., C.K., A.K.K., M.T., and E.S.E. were responsible for data visualization; N.H.T. and E.S.E. provided resources; B.B. and E.S.E. wrote the original draft manuscript; B.B., C.Y.K., A.K.K., M.T., N.D.S., N.H.T., and E.S.E. edited the manuscript; and E.S.E. supervised the study and acquired funding.

Conflict-of-interest disclosure: The authors declare no competing financial interests.

ORCID profiles: B.B., 0000-0001-7780-1744; A.K.K., 0000-0002-2599-131X; M.T., 0000-0003-1900-0652; N.A.P., 0000-0002-4330-5133; N.D.S., 0000-0003-4105-3718; N.H.T., 0000-0002-2689-1337; E.S.E., 0000-0002-2112-7700.

Correspondence: Elizabeth S. Egan, Stanford University School of Medicine, 240 Pasteur Dr, BMI 2400, Stanford, 94305 CA; email: [eeegan@stanford.edu](mailto:eeegan@stanford.edu).

## Footnotes

Submitted 13 April 2023; accepted 30 September 2023; prepublished online on *Blood* First Edition 13 October 2023. <https://doi.org/10.1182/blood.2023020831>.

\*B.B. and C.Y.K. contributed equally to this study.

Original data are available on request from the corresponding author, Elizabeth S. Egan ([eeegan@stanford.edu](mailto:eeegan@stanford.edu)). Proteomics data from the 2-dimensional difference gel electrophoresis and pull-down experiments may be found in data supplements available with the online version of this article. Raw proteomics data can be found at the PRIDE repository.

The online version of this article contains a data supplement.

There is a [Blood Commentary](#) on this article in this issue.

The publication costs of this article were defrayed in part by page charge payment. Therefore, and solely to indicate this fact, this article is hereby marked "advertisement" in accordance with 18 USC section 1734.

## REFERENCES

- World Health Organization. World malaria report 2021. Geneva. 2021.
- Salinas ND, Tang WK, Tolia NH. Blood-stage malaria parasite antigens: structure, function, and vaccine potential. *J Mol Biol*. 2019; 431(21):4259-4280.
- Kumar H, Tolia NH. Getting in: the structural biology of malaria invasion. *PLoS Pathog*. 2019;15(9):e1007943.
- Salinas ND, Tolia NH. Red cell receptors as access points for malaria infection. *Curr Opin Hematol*. 2016;23(3):215-223.
- Malpede BM, Tolia NH. Malaria adhesins: structure and function. *Cell Microbiol*. 2014; 16(5):621-631.
- Paul AS, Egan ES, Duraisingh MT. Host-parasite interactions that guide red blood cell invasion by malaria parasites. *Curr Opin Hematol*. 2015;22(3):220-226.
- Sim BK, Chitnis CE, Wasniowska K, Hadley TJ, Miller LH. Receptor and ligand domains for invasion of erythrocytes by *Plasmodium falciparum*. *Science*. 1994; 264(5167):1941-1944.
- Maier AG, Duraisingh MT, Reeder JC, et al. *Plasmodium falciparum* erythrocyte invasion through glyphorin C and selection for Gerbich negativity in human populations. *Nat Med*. 2003;9(1):87-92.
- Tolia NH, Enemark EJ, Sim BK, Joshua-Tor L. Structural basis for the EBA-175 erythrocyte invasion pathway of the malaria parasite *Plasmodium falciparum*. *Cell*. 2005;122(2): 183-193.
- Mayer DC, Jiang L, Achur RN, Kakizaki I, Gowda DC, Miller LH. The glyphorin C N-linked glycan is a critical component of the ligand for the *Plasmodium falciparum* erythrocyte receptor BAEBL. *Proc Natl Acad Sci U S A*. 2006;103(7):2358-2362.
- Salinas ND, Paing MM, Tolia NH. Critical glycosylated residues in exon three of erythrocyte glyphorin A engage *Plasmodium falciparum* EBA-175 and define receptor specificity. *mBio*. 2014;5(5): e01606-01614.
- Chen E, Paing MM, Salinas N, Sim BK, Tolia NH. Structural and functional basis for inhibition of erythrocyte invasion by antibodies that target *Plasmodium falciparum* EBA-175. *PLoS Pathog*. 2013;9(5):e1003390.
- Malpede BM, Lin DH, Tolia NH. Molecular basis for sialic acid-dependent receptor recognition by the *Plasmodium falciparum* invasion protein erythrocyte-binding antigen-140/BAEBL. *J Biol Chem*. 2013;288(17): 12406-12415.
- Lin DH, Malpede BM, Batchelor JD, Tolia NH. Crystal and solution structures of *Plasmodium falciparum* erythrocyte-binding antigen 140 reveal determinants of receptor specificity during erythrocyte invasion. *J Biol Chem*. 2012;287(44):36830-36836.
- Salinas ND, Tolia NH. A quantitative assay for binding and inhibition of *Plasmodium falciparum* Erythrocyte Binding Antigen 175 reveals high affinity binding depends on

- both DBL domains. *Protein Expr Purif.* 2014; 95:188-194.
16. Tham WH, Healer J, Cowman AF. Erythrocyte and reticulocyte binding-like proteins of *Plasmodium falciparum*. *Trends Parasitol.* 2012;28(1):23-30.
  17. Crosnier C, Bustamante LY, Bartholdson SJ, et al. Basigin is a receptor essential for erythrocyte invasion by *Plasmodium falciparum*. *Nature.* 2011;480(7378):534-537.
  18. Volz JC, Yap A, Sisquella X, et al. Essential role of the PFRh5/PfRipr/CyRPA complex during *Plasmodium falciparum* invasion of erythrocytes. *Cell Host Microbe.* 2016;20(1):60-71.
  19. Scally SW, Triglia T, Evelyn C, et al. PCR complex is essential for invasion of human erythrocytes by *Plasmodium falciparum*. *Nat Microbiol.* 2022;7(12):2039-2053.
  20. Egan ES, Jiang RH, Moechtar MA, et al. Malaria. A forward genetic screen identifies erythrocyte CD55 as essential for *Plasmodium falciparum* invasion. *Science.* 2015;348(6235):711-714.
  21. Kanjee U, Gruring C, Chaand M, et al. CRISPR/Cas9 knockouts reveal genetic interaction between strain-transcendent erythrocyte determinants of *Plasmodium falciparum* invasion. *Proc Natl Acad Sci U S A.* 2017;114(44):E9356-E9365.
  22. Xu Q. The Indian blood group system. *Immunohematology.* 2011;27(3):89-93.
  23. Lux SE. Anatomy of the red cell membrane skeleton: unanswered questions. *Blood.* 2016;127(2):187-199.
  24. Lesley J, Kincade PW, Hyman R. Antibody-induced activation of the hyaluronan receptor function of CD44 requires multivalent binding by antibody. *Eur J Immunol.* 1993;23(8):1902-1909.
  25. Gunthert U, Hofmann M, Rudy W, et al. A new variant of glycoprotein CD44 confers metastatic potential to rat carcinoma cells. *Cell.* 1991;65(1):13-24.
  26. Bourguignon LY, Zhu H, Shao L, Zhu D, Chen YW. Rho-kinase (ROK) promotes CD44v(3,8-10)-ankyrin interaction and tumor cell migration in metastatic breast cancer cells. *Cell Motil Cytoskeleton.* 1999;43(4):269-287.
  27. Morrison H, Sherman LS, Legg J, et al. The NF2 tumor suppressor gene product, merlin, mediates contact inhibition of growth through interactions with CD44. *Genes Dev.* 2001;15(8):968-980.
  28. Ponta H, Sherman L, Herrlich PA. CD44: from adhesion molecules to signalling regulators. *Nat Rev Mol Cell Biol.* 2003;4(1):33-45.
  29. Cywes C, Wessels MR. Group A *Streptococcus* tissue invasion by CD44-mediated cell signalling. *Nature.* 2001; 414(6864):648-652.
  30. Tsukita S, Oishi K, Sato N, Sagara J, Kawai A, Tsukita S. ERM family members as molecular linkers between the cell surface glycoprotein CD44 and actin-based cytoskeletons. *J Cell Biol.* 1994;126(2):391-401.
  31. Legg JW, Lewis CA, Parsons M, Ng T, Isacke CM. A novel PKC-regulated mechanism controls CD44 ezrin association and directional cell motility. *Nat Cell Biol.* 2002;4(6):399-407.
  32. Nam K, Oh S, Lee KM, Yoo SA, Shin I. CD44 regulates cell proliferation, migration, and invasion via modulation of c-Src transcription in human breast cancer cells. *Cell Signal.* 2015;27(9):1882-1894.
  33. Bourguignon LY, Zhu H, Zhou B, Diedrich F, Singleton PA, Hung MC. Hyaluronan promotes CD44v3-Vav2 interaction with Grb2-p185(HER2) and induces Rac1 and Ras signaling during ovarian tumor cell migration and growth. *J Biol Chem.* 2001;276(52):48679-48692.
  34. Orian-Rousseau V, Morrison H, Matzke A, et al. Hepatocyte growth factor-induced Ras activation requires ERM proteins linked to both CD44v6 and F-actin. *Mol Biol Cell.* 2007;18(1):76-83.
  35. Orian-Rousseau V, Chen L, Sleeman JP, Herrlich P, Ponta H. CD44 is required for two consecutive steps in HGF/c-Met signaling. *Genes Dev.* 2002;16(23):3074-3086.
  36. Shen Y, Naujokas M, Park M, Ireton K. InB-dependent internalization of *Listeria* is mediated by the Met receptor tyrosine kinase. *Cell.* 2000;103(3):501-510.
  37. Shakya B, Patel SD, Tani Y, Egan ES. Erythrocyte CD55 mediates the internalization of *Plasmodium falciparum* parasites. *Elife.* 2021;10:e61516.
  38. Suzuki J, Fujita J, Taniguchi S, Sugimoto K, Mori KJ. Characterization of murine hemopoietic-supportive (MS-1 and MS-5) and non-supportive (MS-K) cell lines. *Leukemia.* 1992;6(5):452-458.
  39. Giarratana MC, Kobari L, Lapillonne H, et al. Ex vivo generation of fully mature human red blood cells from hematopoietic stem cells. *Nat Biotechnol.* 2005;23(1):69-74.
  40. Boyle MJ, Wilson DW, Richards JS, et al. Isolation of viable *Plasmodium falciparum* merozoites to define erythrocyte invasion events and advance vaccine and drug development. *Proc Natl Acad Sci U S A.* 2010;107(32):14378-14383.
  41. Paing MM, Salinas ND, Adams Y, et al. Shed EBA-175 mediates red blood cell clustering that enhances malaria parasite growth and enables immune evasion. *Elife.* 2018;7:e43224.
  42. Kurita R, Suda N, Sudo K, et al. Establishment of immortalized human erythroid progenitor cell lines able to produce enucleated red blood cells. *PLoS One.* 2013;8(3):e59890.
  43. Daniels G. *Human Blood Groups*. 3rd ed. John Wiley & Sons, Ltd; 2013.
  44. Sherman LS, Rizvi TA, Karyala S, Ratner N. CD44 enhances neuregulin signaling by Schwann cells. *J Cell Biol.* 2000;150(5):1071-1084.
  45. Bourguignon LY, Zhu H, Chu A, Iida N, Zhang L, Hung MC. Interaction between the adhesion receptor, CD44, and the oncogene product, p185HER2, promotes human ovarian tumor cell activation. *J Biol Chem.* 1997;272(44):27913-27918.
  46. van der Voort R, Taher TE, Wielenga VJ, et al. Heparan sulfate-modified CD44 promotes hepatocyte growth factor/scatter factor-induced signal transduction through the receptor tyrosine kinase c-Met. *J Biol Chem.* 1999;274(10):6499-6506.
  47. Koch M, Wright KE, Otto O, et al. *Plasmodium falciparum* erythrocyte-binding antigen 175 triggers a biophysical change in the red blood cell that facilitates invasion. *Proc Natl Acad Sci U S A.* 2017;114(16):4225-4230.
  48. Sisquella X, Nebel T, Thompson JK, et al. *Plasmodium falciparum* ligand binding to erythrocytes induce alterations in deformability essential for invasion. *Elife.* 2017;6:e21083.
  49. Alloisio N, Dalla Venezia N, Rana A, et al. Evidence that red blood cell protein p55 may participate in the skeleton-membrane linkage that involves protein 4.1 and glycophorin C. *Blood.* 1993;82(4):1323-1327.
  50. Marfatia SM, Lue RA, Branton D, Chishti AH. In vitro binding studies suggest a membrane-associated complex between erythroid p55, protein 4.1, and glycophorin C. *J Biol Chem.* 1994;269(12):8631-8634.
  51. Nunomura W, Takakuwa Y, Parra M, Conboy J, Mohandas N. Regulation of protein 4.1R, p55, and glycophorin C ternary complex in human erythrocyte membrane. *J Biol Chem.* 2000;275(32):24540-24546.
  52. Nunomura W, Takakuwa Y, Tokimitsu R, Krauss SW, Kawashima M, Mohandas N. Regulation of CD44-protein 4.1 interaction by Ca<sup>2+</sup> and calmodulin. Implications for modulation of CD44-ankyrin interaction. *J Biol Chem.* 1997;272(48):30322-30328.
  53. Jeremy KP, Plummer ZE, Head DJ, et al. 4.1R-deficient human red blood cells have altered phosphatidylserine exposure pathways and are deficient in CD44 and CD47 glycoproteins. *Haematologica.* 2009;94(10):1354-1361.
  54. Legg JW, Isacke CM. Identification and functional analysis of the ezrin-binding site in the hyaluronan receptor, CD44. *Curr Biol.* 1998;8(12):705-708.
  55. Jordan AR, Racine RR, Hennig MJ, Lokeshwar VB. The role of CD44 in disease pathophysiology and targeted treatment. *Front Immunol.* 2015;6:182.
  56. Klei TRL, Dalimot JJ, Beuger BM, et al. The Gardos effect drives erythrocyte senescence and leads to Lu/BCAM and CD44 adhesion molecule activation. *Blood Adv.* 2020;4(24):6218-6229.
  57. Dalimot JJ, Klei TRL, Beuger BM, et al. Malaria-associated adhesion molecule activation facilitates the destruction of uninfected red blood cells. *Blood Adv.* 2022; 6(21):5798-5810.
  58. Skoudy A, Mounier J, Aruffo A, et al. CD44 binds to the *Shigella* IpaB protein



- and participates in bacterial invasion of epithelial cells. *Cell Microbiol.* 2000;2(1): 19-33.
59. Wanaguru M, Liu W, Hahn BH, Rayner JC, Wright GJ. RH5-Basigin interaction plays a major role in the host tropism of *Plasmodium falciparum*. *Proc Natl Acad Sci U S A.* 2013; 110(51):20735-20740.
60. Saetear P, Perrin AJ, Bartholdson SJ, et al. Quantification of *Plasmodium*-host protein interactions on intact, unmodified erythrocytes by back-scattering interferometry. *Malar J.* 2015;14:88.
61. Thome RF, Legg JW, Isacke CM. The role of the CD44 transmembrane and cytoplasmic domains in co-ordinating adhesive and signalling events. *J Cell Sci.* 2004;117(Pt 3): 373-380.
62. Adderley JD, John von Freyend S, Jackson SA, et al. Analysis of erythrocyte signalling pathways during *Plasmodium falciparum* infection identifies targets for host-directed antimalarial intervention. *Nat Commun.* 2020;11(1):4015.
63. Chien HD, Pantaleo A, Kesely KR, et al. Imatinib augments standard malaria combination therapy without added toxicity. *J Exp Med.* 2021;218(10):e20210724.
64. Tsamesidis I, Reybier K, Marchetti G, et al. Syk kinase inhibitors synergize with artemisinins by enhancing oxidative stress in *Plasmodium falciparum*-parasitized erythrocytes. *Antioxidants (Basel).* 2020;9(8): 753.
65. Luo Z, Dai Y, Gao H. Development and application of hyaluronic acid in tumor targeting drug delivery. *Acta Pharm Sin B.* 2019;9(6):1099-1112.
66. Kesharwani P, Chadar R, Sheikh A, Rizg WY, Safhi AY. CD44-targeted nanocarrier for cancer therapy. *Front Pharmacol.* 2021;12: 800481.

Licensed under Creative Commons Attribution-NonCommercial-NoDerivatives 4.0 International (CC BY-NC-ND 4.0), permitting only noncommercial, nonderivative use with attribution. All other rights reserved.